Channel Charting Aided Pilot Allocation in Multi-Cell Massive MIMO mMTC Networks

Lucas Ribeiro†, Markus Leinonen†, Isuru Rathnayaka†, Hanan Al-Tous⋆, and Markku Juntti†
†Centre for Wireless Communications, FI-90014, University of Oulu, Finland
⋆Department of Communications and Networking, Aalto University, Finland
e-mail: {lucas.ribeiro, markus.leinonen, markku.juntti}@oulu.fi
isuru.rathnayaka@student.oulu.fi hanan.al-tous@aalto.fi

***Abstract*—Serving a plethora of devices in massive machine-type communications (mMTC) can rely on spatial multiplexing enabled by massive multiple-input multiple-output (mMIMO) technology. To release the full potential, accurate channel estimation is needed. Due to the large numbers of devices it necessitates pilot reuse. We propose a pilot allocation algorithm based on multi-point channel charting (CC) to mitigate inevitable pilot contamination in a multi-cell multi-sector mMTC network with spatially correlated mMIMO channels. The generated CC represents an effective interference map from channel covariance matrices to capture the degree of pilot contamination caused by sharing the same pilot sequence among multiple users. The map is then fed into a greedy algorithm that aims at optimizing the reuse pattern of orthogonal pilot sequences to minimize the performance degradation caused by pilot contamination. The proposed CC-based method is empirically shown to obtain notable gains over a reuse-factor-aware random pilot allocation, yet leaving room for further improvements.**

I. Introduction

Massive multiple-input multiple-output (mMIMO) technology has shown to provide spatial multiplexing gain enabling connecting multiple user equipments (UEs) given that accurate channel state information (CSI) is available at the base stations (BSs) [1]–[3]. However, the large number of devices in massive machine-type communication (mMTC) systems prevents the allocation of *unique* orthogonal pilot sequences to all UEs causing *pilot contamination*, which degrades the accuracy of channel estimates and makes them statistically dependent [4, p. 252]. Therefore, an intelligent strategy to allocate the pilot sequences is needed to avoid or mitigate such a phenomenon.

Lian *et al.* [5] propose a global pilot reuse strategy to reduce pilot overhead and increase spectral efficiency. They developed a greedy algorithm using the UEs' channel covariance matrices to minimize the mean square error (MSE) of the channel estimation by allocating the orthogonal pilot sequences in a coordinated fashion.

A joint mMIMO and non-orthogonal multiple-access (NOMA) approach to mitigate the interference caused by nearby UEs is proposed in [3]. As motivated by Le *et al.* [3], the spatial configuration of UEs is intrinsically related to the interference between them. For finite size antenna arrays, the BS cannot resolve between UEs that are spatially close to each other, which increases the potential source of interference in mMIMO systems. Therefore, they derived a k-means-based algorithm to group UEs based on the chordal distance of their covariance matrices. The results showed that for UEs in such conditions the joint mMIMO-NOMA approach can improve the spectral efficiency.

In [6], *channel charting* (CC) is proposed as a method to capture the slowly varying characteristics of the channels, i.e., large-scale propagation effects into radio environment mappings. CC exploits the spatial information existing in the CSI to create an unsupervised low-dimensional map of UEs, in which the relative positions of UEs are preserved. Preserving the neighborhood information in the low dimensional chart is important as it can be used to identify the spatial orthogonality of the UEs.

In [7]–[9], we showed that CC can be utilized to mitigate pilot contamination and improve the channel estimation accuracy for single-cell setups. In [9], an interference map created using CC was used as an input to a low-complexity pilot allocation algorithm that greedily assigns the pilot sequences. This method showed to increase the channel estimation accuracy as well as the achievable rate.

In this paper, we propose a multi-cell multi-sector interference map to facilitate the assignment of orthogonal pilot sequences in an mMTC network with spatially correlated mMIMO channels. In order to generate a CC map that represents the effective interference between the UEs in the system, we propose a new method to merge the sector's information at the BSs, and then process it at a central processing unit (CPU). The interference map is then utilized by a greedy algorithm to allocate the orthogonal pilot sequences to minimize the performance degradation caused by pilot contamination. Simulation results have shown to improve the accuracy of channel estimates and the symbol error rate (SER) over a reuse-factor-aware random pilot allocation.

II. System model

We consider a multi-cell mMTC mMIMO system, consisting of B BSs, with each cell area split into S sectors. The BSs, each equipped with S M-element uniform linear arrays (ULAs), are connected to a CPU. A set $\mathcal{N} = \{1, \ldots, N\}$ of single-antenna UEs are uniformly distributed across the network as depicted in Fig. 1. To model sporadic user activity in the mMTC traffic, only $K \ll N$ UEs are active at the same transmission interval. We assume a block fading channel model, where the channels are time-invariant and flat fading

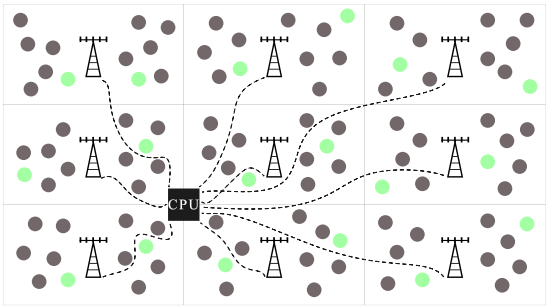

Fig. 1: The considered multi-cell multi-sector mMTC mMIMO network. The circles represent N UEs, out of which only a subset of K UEs are active (green) in a given coherence block.

during one coherence block. A time-division duplex (TDD) protocol is employed such that at the beginning of each coherence block, the set of active UEs, $\mathcal{K} = \{1, \ldots, K\} \subseteq \mathcal{N}$, transmit known pilot symbols to the BS for channel estimation. Herein, we assume that the set of active users are known[1].

We denote the channel between UE n and ULA s at BS b as $\mathbf{h}_{nbs} \in \mathbb{C}^M$. Assuming that the number of multipath components between the UE and ULA tends towards infinity, the channel vector becomes complex Gaussian distributed with zero mean and covariance matrix $\mathbf{R}_{nbs} \in \mathbb{C}^{M \times M}$, i.e., $\mathbf{h}_{nbs} \sim \mathcal{CN}(\mathbf{0}, \mathbf{R}_{nbs})$. Therefore, $\mathbf{h}_{nbs}$ can be modelled as

$$\mathbf{h}_{nbs} = \mathbf{R}_{nbs}^{\frac{1}{2}} \check{\mathbf{e}}, \tag{1}$$

where $\check{\mathbf{e}} \sim \mathcal{CN}(\mathbf{0}, \mathbf{I}_M)$.

The (l, m)th element of the covariance matrix $\mathbf{R}_{nbs}$ can be numerically evaluated for any distribution as [4]

$$[\mathbf{R}_{nbs}]_{l,m} = \beta_{nbs} \int_{-\pi}^{\pi} e^{-j2\pi\Delta_{\mathrm{r}}(l-m)\cos(\theta_{nbs})} f(\theta_{nbs}) d\theta_{nbs} \tag{2}$$

where θ_{nbs} is the angle between UE n and ULA s at BS b, $f(\theta_{nbs})$ is the probability density function (pdf) of the scatterers' distribution around θ_{nbs}, Δ_{r} is the normalized spacing between the antenna elements, and β_{nbs} is average channel gain, which includes the antenna and large-scale propagation effects. The average channel gain is modelled as [4, Eq. 2.3]

$$\beta_{nbs}[\mathrm{dB}] = 35.3 - 37 \log_{10}\left(\frac{d_{nbs}}{1\ \mathrm{m}}\right) + G_{\mathrm{A}}(\theta_{nbs}), \tag{3}$$

where d_{nbs} is the distance in meters from UE n to the ULA s at BS b, and $G_{\mathrm{A}}(\theta_{nbs})$ is the corresponding antenna gain, given as $G_{\mathrm{A}}(\theta_{nbs}) = -\min\left[12\left(\frac{\theta_{nbs}}{\theta_{3\mathrm{dB}}}\right)^2,\ 30\right]$.

According to measurements reported in [14], the pdf of the impinging waves, $f(\theta_{nbs})$, can be modelled as a Gaussian distribution, with most of the scatterers coming from the direction θ_{nbs}, which fits well to the local scattering channel model described in [4, Sec. 2.6]. Here, we assume that the scatterers are uniformly distributed around the nominal angle of arrival $\overline{\theta}_{nbs}$, ranging from $[\overline{\theta}_{nbs} - 3\sigma_\theta, \overline{\theta}_{nbs} + 3\sigma_\theta]$, where σ_θ is the angular standard deviation.

III. Channel Estimation and Data Transmission

A. Uplink Training

We assume that τ *orthogonal* pilot sequences are assigned to the set of N UEs. Because the number of available orthogonal pilot sequences is far smaller than the number of UEs in mMIMO networks, we consider that $\tau \ll N$. *Global* pilot reuse is employed throughout the network in a *centralized* fashion. Let $\mathcal{T} = \{1, \ldots, \tau\}$ be the set of indices of available pilot sequences and $\pi_n \in \mathcal{T}$ be the index of the pilot sequence assigned to UE n. Then, $\boldsymbol{\phi}_{\pi_n} \in \mathbb{C}^\tau$ is the pilot sequence assigned to UE n, which is taken from the orthogonal pilot code book $\boldsymbol{\Phi} = [\boldsymbol{\phi}_1, \ldots, \boldsymbol{\phi}_\tau] \in \mathbb{C}^{\tau \times \tau}$. We denote the group of UEs assigned with the same pilot sequence as UE n, including UE n itself, as $\mathcal{G}_n = \{j \mid j \in \mathcal{N}, \pi_j = \pi_n\}$.

While the pilot allocation is centralized, we consider that the channel estimation is done *locally* at each BS by using (only) sector-level covariance matrices, $\mathbf{R}_{nbs}, \forall n \in \mathcal{N}$. To this end, we assume that the channel covariance matrices of each sector for all UEs (active and inactive ones) are known[2]. In line with this, we will consider local data decoding at each BS, as elaborated in Section III-B. More complex signal processing techniques could be employed to estimate the channels and the received data, such as joint channel estimation among the BSs and sectors, yet at the cost of increased backhaul communication between the BSs and the CPU.

At ULA s of BS b, the received signal from pilot transmission, $\mathbf{Y}_{bs} \in \mathbb{C}^{M \times \tau}$, can be written as

$$\mathbf{Y}_{bs} = \mathbf{H}_{bs}\boldsymbol{\Psi} + \mathbf{N}_{bs}, \tag{4}$$

where $\mathbf{H}_{bs} = [\mathbf{h}_{1bs}, \ldots, \mathbf{h}_{Kbs}] \in \mathbb{C}^{M \times K}$ is the channel matrix for the active UEs, $\mathbf{N}_{bs} \in \mathbb{C}^{M \times \tau}$ is the noise matrix, with entries modelled as i.i.d. zero-mean complex Gaussian with noise power σ_{n}^2, and $\boldsymbol{\Psi} = [\boldsymbol{\psi}_1, \ldots, \boldsymbol{\psi}_K]^{\mathrm{T}} \in \mathbb{C}^{K \times \tau}$ is the pilot signal matrix, obtained from the transmitted pilot sequences after power loading by p_{u}, i.e., $\boldsymbol{\psi}_k = \sqrt{p_{\mathrm{u}}}\boldsymbol{\phi}_{\pi_k}$.

We assume that the linear minimum mean square error (LMMSE) receiver is employed at the BSs to estimate the active UEs' channel vectors for distinct sectors. Therefore, the LMMSE estimate of the channel between user k and the ULA s of BS b, $\hat{\mathbf{h}}_{kbs} \sim \mathcal{CN}(\mathbf{0}, \mathbf{R}_{kbs}\mathbf{Q}_{kbs}^{-1}\mathbf{R}_{kbs})$, is given as [3]

$$\hat{\mathbf{h}}_{kbs} = \mathbf{R}_{kbs}\mathbf{Q}_{kbs}^{-1}\mathbf{y}_{kbs}^{\mathrm{p}}, \tag{5}$$

where $\mathbf{y}_{kbs}^{\mathrm{p}} \in \mathbb{C}^M$ represents the correlated received signal at sector s of BS b for the pilot sequence assigned to user k, i.e.,

$$\mathbf{y}_{kbs}^{\mathrm{p}} = \frac{1}{p_{\mathrm{u}}\tau}\mathbf{Y}_{bs}\boldsymbol{\psi}_k^*, \tag{6}$$

[1]The main focus of this paper is on the channel estimation and developing intelligent pilot allocation to mitigate pilot contamination; several user activity detection algorithms for mMTC have been proposed, see e.g., [10]–[13].

[2]An initial training phase can be used to obtain the first estimates for the covariance matrices (see techniques in, e.g., [2]), which the BS can keep updating at a lower cost, owing to their relatively slow variation.

and $\mathbf{Q}_{kbs} = \mathbb{E}\{\mathbf{y}_{kbs}\mathbf{y}_{kbs}^{\mathrm{H}}\} \in \mathbb{C}^{M\times M}$ is the covariance matrix of the received signal at sector s of BS b, given as

$$\mathbf{Q}_{kbs} = \sum_{j\in\mathcal{G}_k} \mathbf{R}_{jbs} + \frac{\sigma_{\mathrm{n}}^2}{p_{\mathrm{u}}\tau}\mathbf{I}_M. \tag{7}$$

Accordingly, the channel estimation error is independent of $\hat{\mathbf{h}}_{kbs}$ and given by $\tilde{\mathbf{h}}_{kbs} \sim \mathcal{CN}(\mathbf{0}, \mathbf{R}_{\tilde{\mathbf{h}}_{kbs}})$, where $\mathbf{R}_{\tilde{\mathbf{h}}_{kbs}} = \mathbf{R}_{kbs} - \mathbf{R}_{kbs}\mathbf{Q}_{kbs}^{-1}\mathbf{R}_{kbs}$ is the covariance matrix of the channel estimation error.

B. Uplink Data Transmission

The received signal for UE k at sector s and BS b, $\mathbf{y}_{kbs} \in \mathbb{C}^M$, at a given time instant is given by

$$\mathbf{y}_{kbs} = \mathbf{h}_{kbs}x_k + \mathbf{n}_{bs}, \tag{8}$$

where x_k is the transmitted symbol by the kth UE.

The simplest signal detection strategy considering the proposed local signal processing is to assume that each BS selects the signal for UE k from the sector with the largest channel gain and ignores the rest $S-1$ received signals. An analogous strategy to determine the BS serving UE k can be implemented at the CPU to decide on the received symbol for that UE. Thereby, the received symbol for user k can be retrieved as

$$\hat{x}_k = \left(\mathbf{v}_{kb_k^\star s_k^\star}\right)^{\mathrm{H}} \mathbf{y}_{kb_k^\star s_k^\star}, \tag{9}$$

where $\mathbf{v}_{kb_k^\star s_k^\star} \in \mathbb{C}^M$ denotes the receive combiner vector for UE k at sector $s_k^\star$ and BS $b_k^\star$ with the largest received power for that UE, i.e., $[b_k^\star, s_k^\star] = \underset{b\in\mathcal{B},\ s\in\mathcal{S}}{\arg\max}\,(\beta_{kbs})$, where $\mathcal{B} = \{1,\ldots,B\}$ and $\mathcal{S} = \{1,\ldots,S\}$.

The instantaneous uplink signal-to-interference-and-noise ratio (SINR) for UE k is given as [15]

$$\gamma_k = \frac{|\mathbf{v}_{kb_k^\star s_k^\star}^{\mathrm{H}} \hat{\mathbf{h}}_{kb_k^\star s_k^\star}|^2}{\mathbf{v}_{kb_k^\star s_k^\star}^{\mathrm{H}} \left(\sum\limits_{\substack{j\in\mathcal{G}_k \\ j\neq k}} \hat{\mathbf{h}}_{jb_k^\star s_k^\star}\hat{\mathbf{h}}_{jb_k^\star s_k^\star}^{\mathrm{H}} + \sum\limits_{j\prime=1}^{K} \mathbf{R}_{\tilde{\mathbf{h}}_{j\prime b_k^\star s_k^\star}} + \frac{\sigma_{\mathrm{n}}^2}{p_{\mathrm{u}}}\mathbf{I}_M \right) \mathbf{v}_{kb_k^\star s_k^\star}}. \tag{10}$$

As presented in [4, Lemma B.10], the combiner vector $\mathbf{v}_{kb_k^\star s_k^\star}$ which maximizes (10), the instantaneous SINR for UE k, is the LMMSE combiner vector $\mathbf{w}_k \in \mathbb{C}^M$, given by

$$\mathbf{w}_k = \left(\hat{\mathbf{H}}_{b_k^\star s_k^\star}\hat{\mathbf{H}}_{b_k^\star s_k^\star}^{\mathrm{H}} + \sum_{k=1}^{K} \mathbf{R}_{\tilde{\mathbf{h}}_{kb_k^\star s_k^\star}} + \frac{\sigma_{\mathrm{n}}^2}{p_{\mathrm{u}}}\mathbf{I}_{MS} \right)^{-1} \hat{\mathbf{h}}_{kb_k^\star s_k^\star}. \tag{11}$$

IV. CC mapping and Pilot Reuse

Pilot contamination can be very harmful for mMTC systems. As the number of UEs reusing the same pilot sequence increases, the channel estimates become poorer and statistically dependent, which increases the channel estimation error, thereby affecting directly the data transmission phase, as seen in (10). Therefore, a careful assignment of the pilot sequences, when reusing them, is needed to mitigate pilot contamination.

The main target of pilot assignment is to allocate orthogonal pilot sequences to UEs with strong mutual interference. It is known that the interference in such systems is strongly related to the spatial configuration of the UEs and that this relationship is captured by the covariance matrices $\mathbf{R}_{nbs}, \forall n \in \mathcal{N}$ [2]. Therefore, in line with [9], we aim at building a *UE-interference map* to allocate the pilot sequences to mitigate pilot contamination. In Section IV-A, we explain how to obtain the interference map for a multi-cell multi-sector scenario through multi-point CC, whereas Section IV-B describes the pilot allocation strategy using the generated CC map.

A. Multi-cell Multi-sector Channel Charting

To build an interference map of the network, similarly to [9], the covariance matrix distance (CMD) metric [16] is applied to create a dissimilarity matrix $\mathbf{D} = [\mathbf{d}_1, \ldots, \mathbf{d}_N] \in \mathbb{R}^{N\times N}$, where the nth column of $\mathbf{D}$, $\mathbf{d}_n \in \mathbb{R}^N$, represents the feature vector that contains the CMD values of UE n with respect to all N UEs, including n itself. The difference here is that we need to adopt the generation of $\mathbf{D}$ into a multi-cell setting; this will be elaborated next.

Since the sector covariance matrices, $\mathbf{R}_{nbs}$, are assumed to be known at the BSs, they can be used to get the features to generate CC. Hence, the CMD associated with a UE pair n and j seen by ULA s of BS b is given as [16]

$$[\mathbf{D}_{bs}]_{n,j} = 1 - \frac{\mathrm{tr}\left(\mathbf{R}_{nbs}^{\mathrm{H}}\mathbf{R}_{jbs}\right)}{\|\mathbf{R}_{nbs}\|_F\|\mathbf{R}_{jbs}\|_F}, \tag{12}$$

where $\mathbf{D}_{bs}$ is the matrix of features or dissimilarities obtained for sector s of BS b.

To characterize the UEs' geometry in the full extent at the azimuth's domain, each BS has to combine the information from all its sectors. In other words, the set $\mathbf{D}_{bs}, \forall s \in \mathcal{S}$, must be combined into a single per-BS dissimilarity matrix $\mathbf{D}_b \in \mathbb{R}^{N\times N}$. Because of the normalizing factor in (12), the CMD mainly acts as a measure of the UEs' angular distance. Thus, when merging the sector features, one must take into account the effect of *mirror angles* for ULAs [4, p. 258]. This phenomenon has the effect of underestimating the angular distance measured using CMD when UEs are not in the same sector. That would cause UEs to be incorrectly mapped to close positions in the CC interference map, as if they had strong mutual interference. Therefore, our solution adopted herein to avoid misplacing UEs in the CC when the UEs reside in different sectors is to trust the per-sector CMD with the largest value. Therefore, each element of the combined per-BS feature matrix, $\mathbf{D}_b$, is given by

$$[\mathbf{D}_b]_{n,j} = \begin{cases} [\mathbf{D}_{bs_n^\star}]_{n,j}, \text{ if } s_n^\star = s_j^\star; \\ \max\limits_{s\in\mathcal{S}} \left([\mathbf{D}_{bs}]_{n,j}\right), \text{ otherwise.} \end{cases} \tag{13}$$

In [17], a method to merge the local features computed by distinct BSs into a single feature matrix and generate a multi-point CC was proposed. The proposed weighting strategy in [17] takes into account the received power at each BS, where the weight for the measurement between a pair of UEs at a particular BS is proportional to their SNR. Here, we adopt a similar weighting strategy, but instead of using SNR, we use

the large-scale fading coefficients, β_{nbs}, to merge the local feature matrices into one global feature matrix at the CPU. Hence, the global dissimilarity matrix used to generate the UE-interference map is given as

$$[\mathbf{D}]_{n,j} = \frac{1}{\sum_{b=1}^{B} w_b(n,j)} \sum_{b=1}^{B} [\mathbf{D}_b]_{n,j}, \tag{14}$$

where $w_b(n,j) = \min(\beta_{nbs_n^\star}, \beta_{jbs_j^\star})^2$.

After merging the local feature matrices to get $\mathbf{D} \in \mathbb{R}^{N \times N}$, a dimensionality reduction (DR) technique is applied to map the UEs' features to a lower dimensional chart and obtain the desired UE-interference map. As highlighted in [9] and the references therein, several unsupervised DR techniques can be used to generate CC. Thus, we employ t-SNE [18] to get a 3-dimensional UE-interference map: $\mathbf{d}_n \mapsto \mathbf{z}_n$, where $\mathbf{z}_n \in \mathbb{R}^3$ is the coordinate of UE n on that map.

B. Pilot Reuse Strategy

Having generated the interference map through multi-point CC, as presented in Section IV-A, we now employ a pilot reuse strategy that utilizes the map to mitigate pilot contamination. The goal is to assign orthogonal pilot sequences to UEs with potentially strong mutual interference, i.e., UEs that are close in the CC mapping. The proposed CC-based method is an extension of the single-cell pilot reuse method developed in [9] into a multi-cell environment. Thereby, we adopt the *Nearest Neighbor Pilot Assignment Algorithm*, presented in [9], to allocate the pilot sequences using the proposed multi-cell UE-interference map. The goal is to maximize the distance between UEs sharing the same pilot sequence in the CC.

V. Simulation results

We consider $B = 9$ BSs and $N = 450$ UEs uniformly distributed within a 1 km^2 area, where $K = 63$ UEs are simultaneously active, i.e., on average 7 UEs per cell are active at each transmission interval. The BSs are equipped with $S = 3$ ULAs, each with $M = 32$ critically spaced ($\Delta_{\mathrm{r}} = 0.5$) antenna elements. The propagation channel between each UE and the ULA of a BS is modelled according the local scattering model with angular standard deviation $\sigma_\theta = 10^\circ$. The half-power beamwidth is $\theta_{3\mathrm{dB}} = 65^\circ$ [19]. t-SNE with the perplexity parameter fixed to 30 is used as the DR technique. Binary phase shift keying (BPSK) is used for the pilots and quadrature phase shift keying (QPSK) for the data transmission.

Channel estimation accuracy is evaluated in terms of the normalized MSE (NMSE CE), defined as

$$\text{NMSE CE} = \frac{\mathbb{E}\left[\sum_{k=1}^{K} \|\hat{\mathbf{h}}_{kb_k^\star s_k^\star} - \mathbf{h}_{kb_k^\star s_k^\star}\|^2\right]}{\mathbb{E}\left[\sum_{k=1}^{K} \|\mathbf{h}_{kb_k^\star s_k^\star}\|^2\right]}, \tag{15}$$

where the expectation is evaluated through Monte Carlo simulations. For data decoding, we use the LMMSE receiver in (11) and evaluate the resulting symbol error rate (SER).

The following baselines are considered.

- "Orthogonal": Orthogonal pilot allocation that allocates unique orthogonal pilot sequences of length N to the UEs. To have a fair comparison, we compensate for the longer sequence by normalizing the powers of the orthogonal sequences to match the pilot sequence power used by the other methods, $p_{\mathrm{u}}\tau$.
- "Random": A reuse-factor-aware random allocation that assigns the orthogonal pilot sequences uniformly at random, while ensuring that the same pilot sequence is reused the minimum required times in the network.
- "CMD": The CMD-aided pilot assignment method proposed in [8], which employs the proposed greedy pilot allocation algorithm directly for the feature matrix, $\mathbf{D}$ in (14), without using any DR technique.
- "CPR": Coordinated pilot reuse (CPR) proposed in [5] that aims at minimizing the MSE CE. Similar to our method, it uses second-order statistics to allocate the pilot sequences. To adapt the method into our multi-sector setup, we block-diagonalized the sector-level covariance matrices before feeding it to the algorithm.

Fig. 2 shows the impact of SNR on the performance of the different pilot reuse algorithms in terms of (a) NMSE CE and (b) SER. Fig. 2(a) highlights that the benefits of an intelligent pilot allocation are more evident at high SNR regimes, where the interference is more detrimental than noise. For $\tau = 16$, the proposed method and CMD-based pilot allocation show improvement in channel estimation accuracy, about 2.5 and 2 dB lower NMSE CE over random pilot allocation, respectively, whereas the CPR method showed almost 6 dB gain for the same setup. As a SER benchmark for all methods, we also depict "Lower bound", achieved by considering perfect CSI knowledge in the LMMSE receiver combining. Using the instantaneous-SINR-optimal receive combiner in (11), we observe that SER for the CC-based method gets very close to that of CPR. However, one should expect seeing lower SER with better channel estimation accuracy. Thus, suggesting that one could employ a more efficient combiner structure for the SER. We further notice that SER for the orthogonal pilot allocation performs almost as good as the perfect CSI lower bound, approaching it as SNR increases.

Fig. 3 shows the impact of pilot sequence length τ on the NMSE CE performance for different pilot reuse algorithms at 20 dB SNR. We can see that for small pilot sequence length, around $\tau = 8$, the performance for all methods gets closer to random pilot allocation, whereas for smaller pilot reuse factors, the proposed method improves about 2.5 dB over the random assignment. However, as τ increases, the proposed method improves the channel estimate accuracy at a similar rate of random pilot allocation, whereas CPR method shows larger gains over random strategy.

VI. Conclusions

We proposed a multi-point CC approach for pilot reuse to mitigate pilot contamination in a multi-cell multi-sector mMTC network with spatially correlated mMIMO channels. The proposed method creates a network-wide UE-interference map that facilitates the pilot assignment, which is infeasible to obtain optimally for a large number of UEs, such as in mMTC

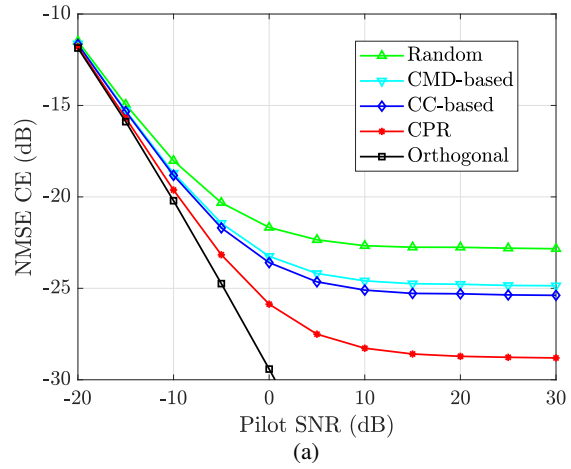

(a)

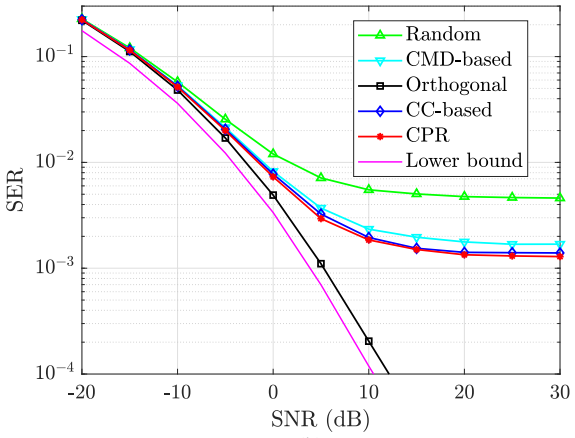

(b)

Fig. 2: Performance of the proposed CC-based pilot reuse algorithm in comparison to the baselines as a function of SNR in (dB) using: (a) NMSE CE (b) SER.

systems. Numerical results showed that the proposed CC-based method considerably suppresses the pilot contamination compared to a reuse-factor-aware random pilot allocation, yet revealing that the CC approach could be further optimized. Future studies on more sophisticated pilot allocation algorithms that rely on the UE-interference map could be a path to follow to improve the performance of the proposed method.

VII. Acknowledgements

This research has been financially supported by the Academy of Finland under the projects ROHM and 6G Flagship. The work of M. Leinonen has also been financially supported in part by the Academy of Finland (grant 340171).

References

[1] T. L. Marzetta, "Noncooperative cellular wireless with unlimited numbers of base station antennas," *IEEE Trans. Wireless Commun.*, vol. 9, no. 11, pp. 3590–3600, 2010.

[2] L. Sanguinetti, E. Björnson, and J. Hoydis, "Toward massive MIMO 2.0: Understanding spatial correlation, interference suppression, and pilot contamination," *IEEE Trans. Commun.*, vol. 68, no. 1, pp. 232–257, 2020.

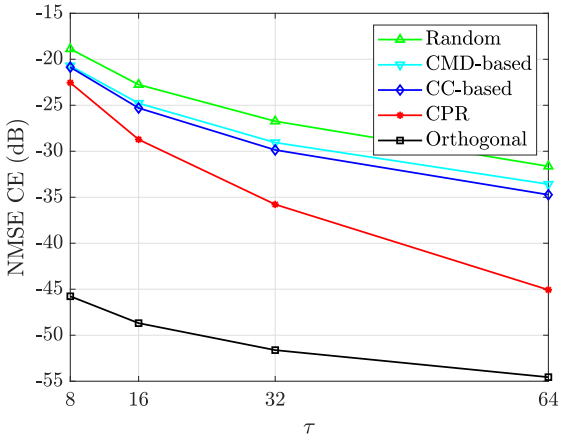

Fig. 3: Effect of pilot length τ on NMSE CE at 20 dB SNR.

[3] M. T. P. Le, L. Sanguinetti, E. Björnson, and M.-G. D. Benedetto, "Code-domain NOMA in massive MIMO: When is it needed?" *IEEE Trans. Veh. Technol.*, vol. 70, no. 5, pp. 4709–4723, 2021.

[4] E. Björnson, J. Hoydis, and L. Sanguinetti, "Massive MIMO networks: Spectral, energy, and hardware efficiency," *Found. Trends Signal Proc.*, vol. 11, no. 3-4, pp. 154–655, 2017.

[5] T. Lian, L. You, W. Zhong, and X. Gao, "Coordinated pilot reuse for multi-cell massive MIMO transmission," in *Proc. IEEE Int. Symp. Pers., Indoor, Mobile Radio Commun.*, 2014, pp. 492–496.

[6] C. Studer, S. Medjkouh, E. Gonultaş, T. Goldstein, and O. Tirkkonen, "Channel Charting: Locating users within the radio environment using channel state information," *IEEE Acc.*, vol. 6, pp. 47 682–47 698, 2018.

[7] L. Ribeiro, M. Leinonen, H. Djelouat, and M. Juntti, "Channel charting for pilot reuse in mMTC with spatially correlated MIMO channels," in *Proc. IEEE Global Telecommun. Conf. Worksh.*, 2020, pp. 1–6.

[8] L. Ribeiro, M. Leinonen, H. Al-Tous, O. Tirkkonen, and M. Juntti, "Exploiting spatial correlation for pilot reuse in single-cell mMTC," in *Proc. IEEE Int. Symp. Pers., Indoor, Mobile Radio Commun.*, 2021.

[9] L. Ribeiro, M. Leinonen, H. Al-Tous, O. Tirkkonen, and M. Juntti, "Pilot reuse for mMTC with spatially correlated MIMO channels: A channel charting approach," *arXiv:2203.06651*, 2022.

[10] Z. Chen, F. Sohrabi, and W. Yu, "Sparse activity detection for massive connectivity," *IEEE Trans. Signal Processing*, vol. 66, no. 7, pp. 1890–1904, 2018.

[11] K. Senel and E. G. Larsson, "Grant-free massive MTC-enabled massive MIMO: A compressive sensing approach," *IEEE Trans. Commun.*, vol. 66, no. 12, pp. 6164–6175, 2018.

[12] H. Djelouat, M. Leinonen, L. Ribeiro, and M. Juntti, "Joint user identification and channel estimation via exploiting spatial channel covariance in mMTC," *IEEE Wireless Commun. Lett.*, pp. 1–1, 2021.

[13] H. Djelouat, M. Leinonen, and M. Juntti, "Spatial correlation aware compressed sensing for user activity detection and channel estimation in massive MTC," *IEEE Trans. Wireless Commun.*, pp. 1–1, 2022.

[14] K. Pedersen, P. Mogensen, and B. Fleury, "A stochastic model of the temporal and azimuthal dispersion seen at the base station in outdoor propagation environments," *IEEE Trans. Veh. Technol.*, vol. 49, no. 2, pp. 437–447, 2000.

[15] L. You, X. Gao, X. Xia, N. Ma, and Y. Peng, "Massive MIMO transmission with pilot reuse in single cell," in *Proc. IEEE Int. Conf. Commun.*, 2014, pp. 4783–4788.

[16] M. Herdin, N. Czink, H. Ozcelik, and E. Bonek, "Correlation matrix distance, a meaningful measure for evaluation of non-stationary MIMO channels," in *Proc. IEEE Veh. Technol. Conf.*, vol. 1, 2005, pp. 136–140.

[17] H. Al-Tous, S. Ponnada, C. Studer, and O. Tirkkonen, "Multipoint channel charting-based radio resource management for V2V communications," *EURASIP J. Wireless Comm. and Netw.*, vol. Volume 2020, issue 1, 2020.

[18] L. van der Maaten and G. Hinton, "Visualizing data using t-sne," *Journal of Machine Learning Research*, vol. 9, no. 86, pp. 2579–2605, 2008.

[19] 3GPP, "Technical specification group radio access network; study on 3D channel model for LTE," V12.7.0.